Available online at www.sciencedirect.com

ScienceDirect

Trans. Nonferrous Met. Soc. China 22(2012) 489−495

Transactions of Nonferrous Metals Society of China

www.tnmsc.cn

Effect of extrusion process on microstructure and mechanical properties of Ni_3Al−B−Cr alloy during self-propagation high-temperature synthesis

SHENG Li-yuan[1, 2], XI Ting-fei[1], LAI Chen[1], GUO Jian-ting[3], ZHENG Yu-feng[2]

1. PKU-HKUST Shenzhen−Hong Kong Institution, Shenzhen 518057, China;
2. College of Engineering, Peking University, Beijing 100871, China;
3. Institute of Metal Research, Chinese Academy of Sciences, Shenyang 110016, China

Received 9 September 2011; accepted 16 January 2012

Abstract: The well-densified Ni_3Al−0.5B−5Cr alloy was fabricated by self-propagation high-temperature synthesis and extrusion technique. Microstructure examination shows that the synthesized alloy has fine microstructure and contains Ni_3Al, Al_2O_3, Ni_3B and Cr_3Ni_2 phases. Moreover, the self-propagation high-temperature synthesis and extrusion lead to great deformation and recrystallization in the alloy, which helps to refine the microstructure and weaken the misorientation. In addition, the subsequent extrusion procedure redistributes the Al_2O_3 particles and eliminates the γ-Ni phase. Compared with the alloy synthesized without extrusion, the Ni_3Al−0.5B−5Cr alloy fabricated by self-propagation high-temperature synthesis and extrusion has better room temperature mechanical properties, which should be ascribed to the microstructure evolution.

Key words: Ni_3Al intermetallic compound; self-propagation high-temperature synthesis; extrusion; microstructure; mechanical properties

---

1 Introduction

Nickel aluminide intermetallic alloys (NiAl and Ni_3Al) have received considerable attention for high-temperature structural and coating applications, e.g., as heat shields for combustion chambers and as first-row vanes in industrial gas turbines [1,2]. In addition, numerous alloys based upon Ni_3Al have been developed with broad utilizations ranging from furnace rolls and radiant burner tubes for steel production to heat treating fixtures, forging dies, and corrosion-resistant parts for chemical industries [3,4]. This is because strong bonding between aluminum and nickel, which persists at elevated temperatures, yields excellent properties competitive with those of superalloys and ceramics, such as high melting point, low densities, high strength, as well as good corrosion and oxidation resistance [1−4]. In spite of these attractive properties, however, low ductility, brittle fracture, and processing problems were the major disadvantages of nickel aluminides [3−5]. The brittleness of Ni_3Al stems from an environmental effect caused by hydrogen generated through the reduction of moisture in air by aluminum in the aluminides [4,6]. A major breakthrough to resolve this issue is the discovery of the dramatic effects of boron addition on ductility improvement for Ni_3Al at ambient and high temperatures. LIU et al [7] found that 50% tensile ductility can be achieved in the Ni_3Al alloy with the addition of small amount of boron up to 0.4%. Interestingly, as the Al content of B-doped Ni_3Al is decreased to below 25% (mole fraction), the ductility increases significantly and the fracture mode changes from brittle intergranular to ductile transgranular. However, the ductility drops drastically to about 5% when the Al content is increased to 25% (mole fraction) or higher.

MORSI [1] reviewed a number of novel processes applied to the reaction synthesis of Ni−Al intermetallics. Among them, combustion synthesis with the advantages of time and energy savings has been recognized as a promising alternative to the conventional methods of producing advanced materials, including carbides,

---

Foundation item: Project (2012CB933600) supported by the National Basic Research Program of China; Project (2011AA030104) supported by the National High-tech Research and Development Program of China; Project (JC200903170498A) supported by the Science and Technology Research Foundation of Shenzhen Bureau of Science and Technology & Information, China

Corresponding author: SHENG Li-yuan; Tel: +86-18665806226; Fax: +86-755-26984814; Email: lysheng@yeah.net

DOI: 10.1016/S1003-6326(11)61203-X

borides, nitrides, hydrides, and intermetallics, etc [8−11]. Combustion synthesis of the Ni_3Al intermetallic can be conducted in either of two modes, the self-propagating high-temperature synthesis (SHS) [12,13] and the thermal explosion [14,15]. By using combustion synthesis in the SHS mode with powder compacts, LEBRAT and VARMA [13] found that higher green density and preheating temperature led to fully reacted product with a well-developed microstructure.

Though the synthesis of Ni_3Al has been extensively studied, the porosity is still its main problem. The hot extrusion could solve the trouble, but it resulted in the crystal coarsening. The recent studies [12,13] reveal that the combustion synthesis and hot extrusion can get well-densified materials. Therefore, in the present work, the Ni_3Al−0.5B−5Cr (Ni_3Al−B−Cr for short) alloy was fabricated by SHS with and without extrusion, and their microstructure and mechanical properties were investigated.

2 Experimental

Two kinds of powders, including powders of nickel (with an average particle size of 0.98 μm) and aluminum (1.45 μm) were used as the initial materials. Besides the main constituents, boron powders (3 μm) and chromium powders (0.92 μm) were used as the additive. Powder mixtures with nominal composition ($n(\mathrm{Ni}):n(\mathrm{Al}):n(\mathrm{Cr}):n(\mathrm{B})=71:23.5:5:0.5$) were dry mixed in a ball milling for 10 h. The mixed powders were compacted into a cylinder with dimensions of *d*40 mm×40 mm, and then the powder compact was put into the SHS with extrusion synthesis system, as shown in Fig. 1(a). Firstly, the induction coil heated the reaction puncheon rapidly to 760 K to start the reaction synthesis. A thermocouple in the SHS synthesis system was used to measure the temperature of the powder mixtures. When the temperature increased dramatically, it signaled the start of reaction synthesis. Then, two seconds later, a pressure of 400 MPa would load on the reaction puncheon in order to extrude the synthesized Ni_3Al out of the reaction floor through a hole with diameter of 6 mm. The as-fabricated sample is shown in Fig. 1(b). In order to investigate the effect of the extrusion, a sample without extrusion was fabricated in the present work.

The specimens for microstructure observation and compression test were cut from the center of the extruded part in sample with hot extrusion and the centre of the sample without extrusion. The resultant phases in the different alloys were characterized by X-ray diffraction (XRD) with a Cu K_α radiation at 40 kV and 40 mA. Microstructural characterizations of all samples were carried out on an OLYMPUS GX41 optical microscope (OM). Samples for OM observations were prepared by conventional methods of mechanical polishing and chemical etching with an acidic mixture ($V(\mathrm{CH_3COOH}):V(\mathrm{HNO_3}):V(\mathrm{HCl})=8:4:1$). The foils for transmission electron microscopy (TEM) observation were prepared by the conventional twin jet polishing technique using an electrolyte of 10% perchloric acid in methnol at –20 °C after mechanically polishing to 50 μm and cutting into disc with a diameter of 3.0 mm. The TEM observation was performed on a JEM−2010 transmission electron microscope operated at 200 kV.

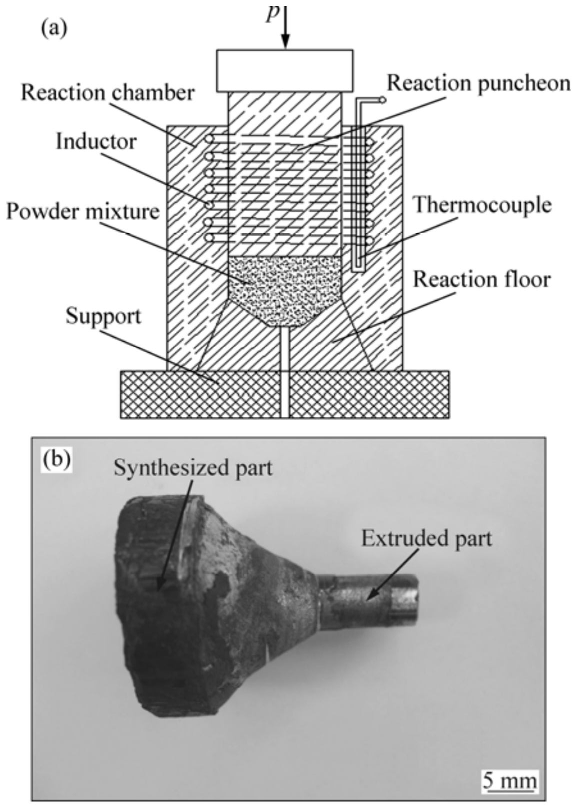

Fig. 1 Schematic diagram of self-propagation high-temperature synthesis and extrusion synthesis system (a), and appearance of synthesized sample by SHS with extrusion (b)

Microhardness measurement was carried out on a Vickers microhardness tester (MHV−2000) using a load of 1.47 N and a dwell time of 15 s. Seven measurements were performed to evaluate an average value. The compressive specimens with dimensions of 4 mm×4 mm×6 mm were cut from the samples and all surfaces were mechanically ground with 600-grit SiC abrasive prior to compression test. The compression was conducted on a Gleeble−1500 test machine at room temperature (RT), with an initial strain rate of 1×10^{-3} s^{-1}.

3 Results and discussion

3.1 Microstructure

X-ray diffraction patterns reveal that the elemental powders were transformed to the Ni_3Al phase after SHS processing, as shown in Fig. 2. From the XRD pattern of the sample without extrusion, it can be seen that the B and Cr additions have not led to any changes. There is no any other phase except the Ni_3Al. However, the extrusion subsequent following the SHS exerts great influence on the microstructure. The extrusion leads to the great increase of [111] peak, which indicates that the sample has a strong tendency along [111]. In addition, it also shows that there are obvious peaks of Al_2O_3, Cr_3Ni_2 and Ni_3B phases, and moreover the peak of Al_2O_3 is strong. Such a difference should be mainly attributed to the great deformation and the short ageing time caused by the residual heat. Based on the previous research [16], the complex effect of ageing and great deformation can promote the precipitation.

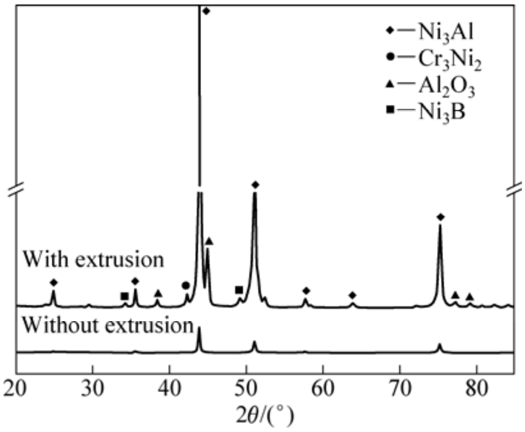

Fig. 2 X-ray diffraction patterns of Ni_3Al−B−Cr alloy synthesized by SHS with and without extrusion

The microstructures of all samples prepared by SHS with and without extrusion are shown in Fig. 3. It is clear that the sample without hot extrusion still has big cavity, and has coarse and fine grains simultaneously with size from 2 to 40 μm, as shown in Fig. 3(a). Twinned Ni_3Al crystals are easy to be found in the sample without extrusion. The Al_2O_3 dispersoids segregate along the Ni_3Al grain boundary. The sample with extrusion exhibits fine and homogeneous grain size and less porosity, as shown in Fig. 3(b). Compared with the sample without extrusion, it can be found that the amount of Al_2O_3 in the sample with extrusion increases a little, and these Al_2O_3 dispersoids prefer to aggregate and distribute along the grain boundary. The origin of Al_2O_3 dispersoids can be explained by either the fracture of the oxide layer covering the original powder particles or powder oxidation during the milling process. The formation of Al_2O_3 dispersoids and their effect on the formation of a microstructure with coarse and fine grains have been explained elsewhere [12,13].

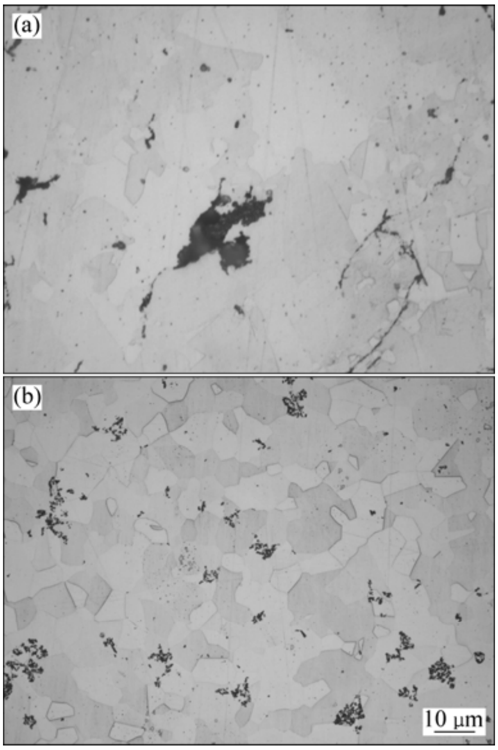

Fig. 3 Optical micrographs of Ni_3Al−B−Cr alloy synthesized by SHS: (a) Without extrusion, (b) With extrusion

The results of TEM observations on the sample without extrusion are presented in Fig. 4. It is clear that the sample is mainly composed of Ni_3Al phase, but it still consists of other phases, as shown in Fig. 4(a). The γ-Ni phase with size of several micrometers exists in the sample, which may be ascribed to the elements segregation. Additionally, the α-Cr particles with hundreds of nanometers are observed in the Ni_3Al matrix, as shown in Fig. 4(b). Based on the recent study [17], the amount of Cr addition in the present work is less than its solubility in Ni_3Al. Therefore, the precipitation of α-Cr particles should be attributed to the relatively low cooling rate, according to the previous research [18]. In addition, the Al_2O_3 particle is observed along Ni_3Al grain boundary, as shown in Fig. 4(c). The inset selected area electron diffraction (SAED) pattern reveals that it is θ-Al_2O_3. The existence of such a metastable phase may be explained by relatively rapid synthesis process, which handicaps its transformation. The TEM observations also certify the twinned Ni_3Al crystal, as shown in Fig. 4(d). Previous research has exhibited that the annealing treatment on high-deformed Ni_3Al polycrystals can lead to the formation of twinned Ni_3Al [18]. In the present investigation, the pre-compaction can generate great stress in the sample, which may contribute to the formation of the twinned Ni_3Al.

TEM observations on the sample with hot extrusion reveal that ultrafine Ni_3Al grains with hundreds nanometers exist in the extruded part, as shown in Fig. 5(a). Along the Ni_3Al grain boundary, the Cr_3Ni_2 precipitate is observed, as shown in Fig. 5(b). According to the recent research [17], such a phase would precipitate in a short ageing time. So, it can be deduced that the great stress and relatively low cooling rate at moderate temperature promote the formation of Cr_3Ni_2 phase. Moreover the small Ni_3B particle is observed in the extruded part, as shown in Fig. 5(c). Further observations along the Ni_3Al grain boundary reveal that the Al_2O_3 particles segregate, as shown in Fig. 5(d). The evolution of the sample with hot extrusion compared with the sample without hot extrusion should mainly attribute to the great deformation, which promotes the microstructure refinement and element diffusion.

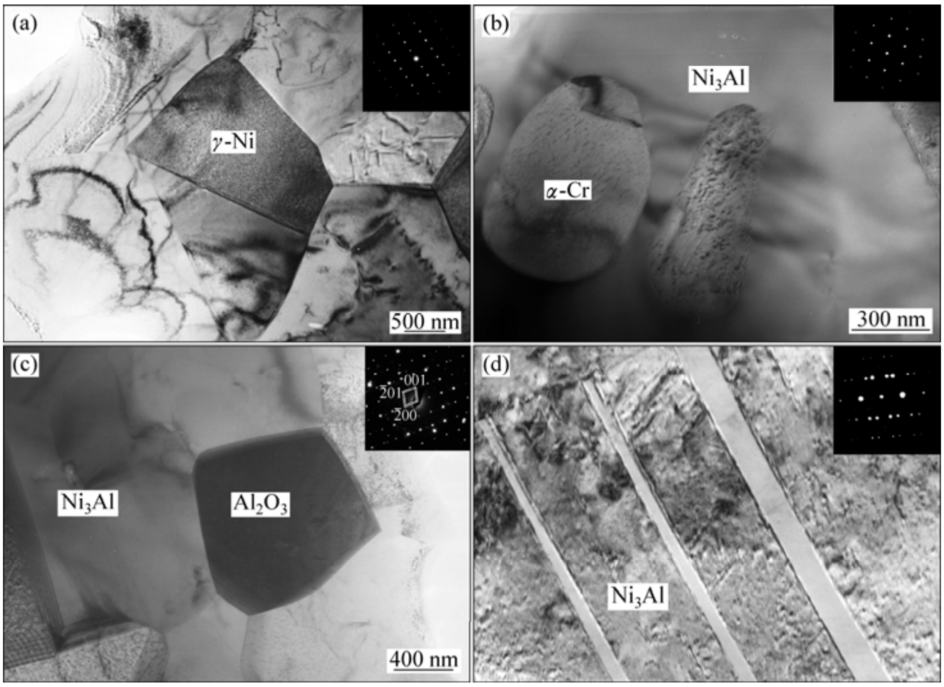

Fig. 4 TEM bright-field images of Ni_3Al−B−Cr alloy synthesized by SHS without extrusion: (a) Morphology of *γ*-Ni in matrix; (b) Precipitation of *α*-Cr-rich particle in Ni_3Al grain; (c) Formation of *θ*-Al_2O_3 along grain boundary; (d) Morphology of twinned Ni_3Al (Insets show SAED patterns of corresponding phases)

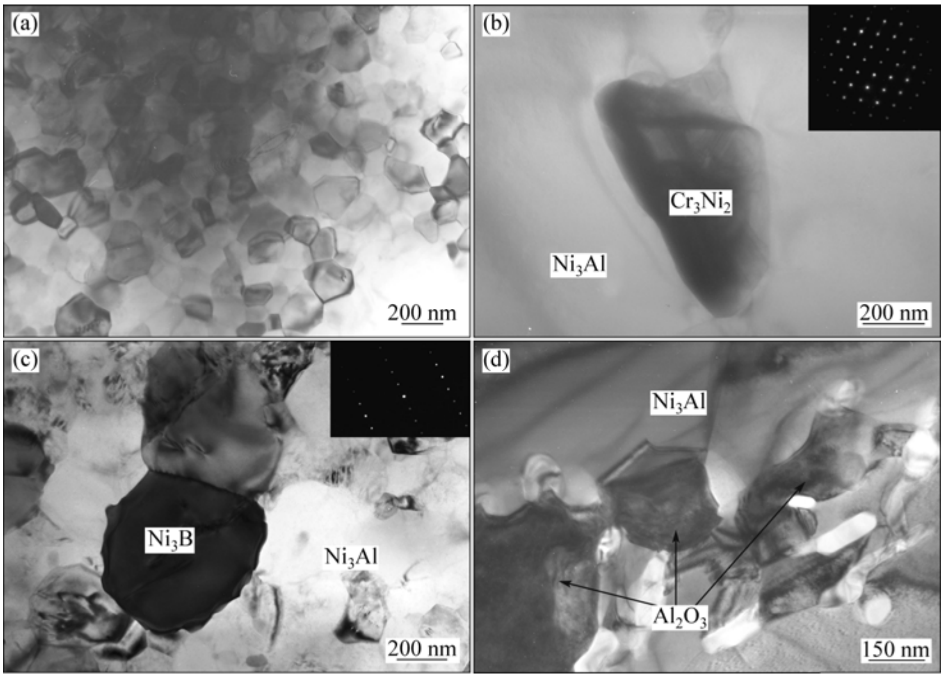

Fig. 5 TEM bright-field images of Ni_3Al−B−Cr alloy synthesized by SHS with extrusion: (a) Morphology of ultrafine Ni_3Al in extruded part; (b) Precipitation of Cr_3Ni_2 phase along Ni_3Al grain boundary; (c) Formation of Ni_3B precipitate in fine Ni_3Al region; (d) Segregation of fine Al_2O_3 particles along Ni_3Al grain boundary (Insets show SAED patterns of corresponding phases)

Further observations on the Al_2O_3 in the extruded part reveal that the Al_2O_3 particles have two different kinds of structures. The morphology of the Al_2O_3 particles and their selected area electron diffraction (SAED) patterns are exhibited in Fig. 6. One has the hexagonal crystal structure with $R\bar{3}c$ space group and the cell parameters: $a=b=0.4758$ nm, $c=1.299$ nm, as shown in Figs. 6(a)−(c). This Al_2O_3 can be determined as α-Al_2O_3, which is the most stable one in all Al_2O_3. The other one has the face-centered crystal structure with $Fd\bar{3}m$ space group and cell parameters: $a=b=c=0.7948$ nm, as shown in Figs. 6(d)−(e). This Al_2O_3 is determined as the γ-Al_2O_3, which is a metastable phase and will transform into α-Al_2O_3 when heat-treated above 1200 K. The existence of the two kinds of Al_2O_3 should be attributed to the synthesis process. The high pressure and rapid heating process lead to the formation of Al_2O_3 with different structures, while the short time at high temperature keeps the structure of the Al_2O_3.

The difference between these two kinds of samples is the extrusion procedure after the self-propagation high-temperature synthesis. The morphology of the extruded part of the sample with the extrusion is shown in Fig. 7(a). It is obvious that the Ni_3Al matrix deforms drastically. The Ni_3Al grains are elongated along the extrusion direction. Compared with the sample without hot extrusion, the size of the Ni_3Al grains in the extruded part is refined significantly. From the results it can be concluded that the Ni_3Al grains are fragmentized and then recrystallized in the following process. But due to the short time at high temperature, the recrystallization is incomplete. So, in the extruded part there are massive dislocations in many Ni_3Al grains, which result in many substructures. As shown in Fig. 7(b), the dislocations in the big Ni_3Al grain have regular array, which indicates the deformation crystal plane. While in the small Ni_3Al grain, the dislocations interact and accumulate in the grain boundary, as shown in Fig. 7(c).

3.2 Mechanical properties

The microhardness and compressive properties at room temperature (RT) of the samples with and without

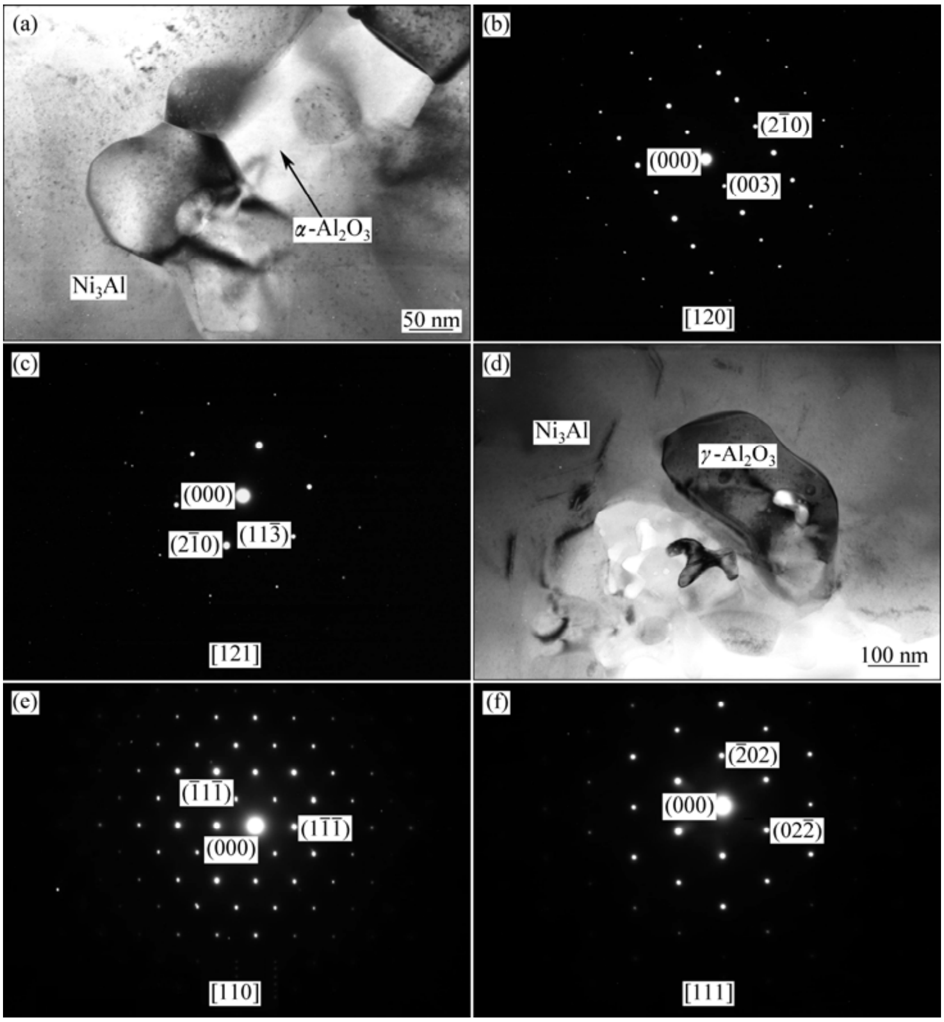

Fig. 6 TEM images of α-Al_2O_3 particle (a) and SAED patterns along [120] (b) and [121] (c), TEM micrograph of γ-Al_2O_3 particle (d) and SAED patterns along [110] (e) and [111] (f)

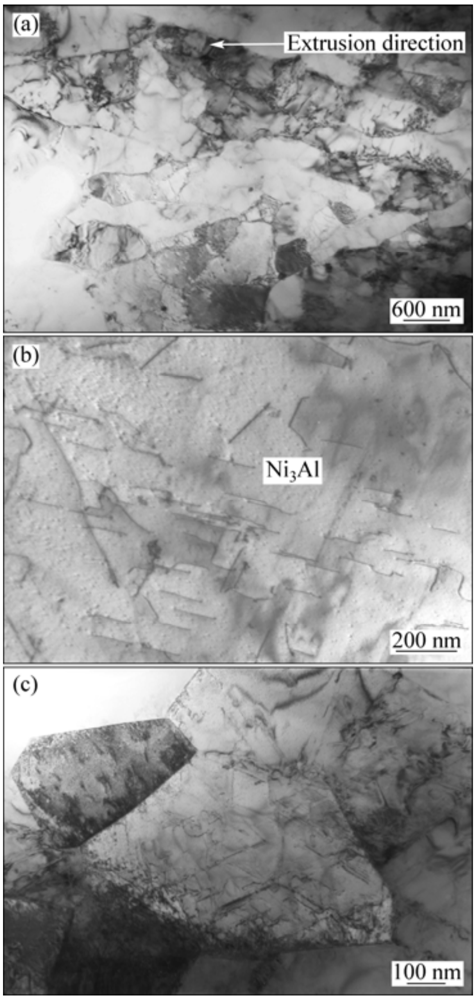

Fig. 7 TEM images of extruded part: (a) Deformed grains along extrusion direction; (b) Morphology of dislocation array in Ni_3Al matrix; (c) Morphology of dislocations in fine Ni_3Al grain

extrusion are shown in Table 1. It is clear that the mechanical properties of the sample with extrusion are better than those of the sample without extrusion. Especially the compressive strain increases by more than 50%, compared with the sample without extrusion. The hardness and strength of the sample with extrusion increase by 15%−25%. The previous studies [19,20] on the Ni_3Al find that the grain size has great effect on the yield strength and its ductility. With the decrease of grain size, the yield strength and ductility at room temperature of the Ni_3Al increase obviously. In the present investigation, the extrusion following the SHS refines the Ni_3Al. It can be believed that it would improve the yield strength of the Ni_3Al further. Additionally, the TEM observation on the extruded part shows a lot of dislocations generated from the grain boundary. According to the researches [21,22], these dislocations act as sources for emitting matrix dislocations, which would improve the ductility and fracture toughness of the materials.

Table 1 Mechanical properties of samples prepared by SHS with and without extrusion at room temperature

Sample	Microhardness (HV)	Yield strength/ MPa	Compressive strength/ MPa	Compressive strain/%
Without extrusion	450	725	1475	35
With extrusion	570	850	1660	55

Previous research [23] on the Ni_3Al revealed that great deformation could result in microcrystalline with high density of defects (dislocations, twins, slip bands) by fragmentation, mechanical twinning of the initial crystals. In the present investigation, the extrusion process after the SHS leads to great deformation in the Ni_3Al−B−Cr alloy. Based on the above observation, it can be concluded that the great pressure extrudes the synthesized alloy out. During the extrusion procedure, a funnel-shaped flowing zone is formed and the funnel-shaped flowing zone results in the break of the bulk Ni_3Al grain into microcrystalline. Moreover, the microcrystalline is twisted at the end of the funnel-shaped flowing zone, which makes the microcrystalline have weak misorientation. At last, the extruded Ni_3Al with homogeneous and fine microstructure and less porosity is obtained, which improves its mechanical properties significantly. In addition, the dispensed Al_2O_3 oxides along the grain boundary contribute to the fragmentation of massive grains. In return, the fragmentation makes the Al_2O_3 oxides distribute more uniformly, which is beneficial to the strength and ductility. Therefore, it can be seen that the sample with extrusion has better mechanical properties.

4 Conclusions

1) The self-propagation high-temperature synthesis and subsequent extrusion densify the Ni_3Al−0.5B−5Cr alloy and refine the microstructure obviously.

2) Besides the Ni_3Al, the alloy synthesized by self-propagation high-temperature synthesis still contains θ-Al_2O_3, γ-Ni, α-Cr and NiAl particles. While in the alloy synthesized by self-propagation high-temperature synthesis and extrusion, α-Al_2O_3, γ-Al_2O_3, Cr_3Ni_2 and Ni_3B particles become the main precipitates.

3) The alloy synthesized by self-propagation high-temperature synthesis and extrusion experiences great deformation and recrystallization, which contributes to the microstructure refinement and weakens the misorientation.

4) Compared with the synthesized alloy without hot extrusion, the self-propagation high-temperature

synthesis and extrusion improve the Ni$_3$Al−0.5B−5Cr alloy obviously, especially the ductility, which increases by almost 60%.

References

[1] MORSI K. Review: Reaction synthesis processing of Ni−Al intermetallic materials [J]. Materials Science and Engineering A, 2001, 299(1−2): 1−15.

[2] SCHEPPE F, SAHM P R, HERMANN W, PAUL U, PREUHS J. Nickel aluminides: A step toward industrial application [J]. Materials Science and Engineering A, 2002, 329−331: 596−601.

[3] STOLOFF N S, LIU C T, DEEVI S C. Emerging applications of intermetallics [J]. Intermetallics, 2000, 8(9−11): 1313−1320.

[4] SIKKA V K, DEEVI S C, VISWANATHAN S, SWINDEMAN R W, SANTELLA M L. Advances in processing of Ni$_3$Al-based intermetallics and applications [J]. Intermetallics, 2000, 8(9−11): 1329−1337.

[5] DEEVI S C, SIKKA V K. Nickel and iron aluminides: an overview on properties, processing, and applications [J]. Intermetallics, 1996, 4(5): 357−375.

[6] GEORGE E P, LIU C T, POPE D P. Intrinsic ductility and environmental embrittlement of binary Ni$_3$Al [J]. Scripta Metall Mater, 1993, 28(7): 857−862.

[7] LIU C T, WHITE C L, HORTON J A. Effect of boron on grain-boundaries in Ni$_3$Al [J]. Acta Metall, 1985, 33(2): 213−229.

[8] MUNIR Z A, ANSELMI-TAMBURINI U. Self-propagating exothermic reactions: The synthesis of high-temperature materials by combustion [J]. Materials Science Reports, 1989, 3(6): 277−365.

[9] MERZHANOV A G. History and recent developments in SHS [J]. Ceramics International, 1995, 21(5): 371−379.

[10] MOORE J J, FENG H J. Combustion synthesis of advanced materials: Part I. Reaction parameters [J]. Progress in Materials Science, 1995, 39(4−5): 243−273.

[11] MOSSINO P. Some aspects in self-propagating high-temperature synthesis [J]. Ceramics International, 2004, 30(3): 311−332.

[12] GUO J T, SHENG L Y, XIE Y, ZHANG Z X, OVCHARENKO V E, YE H Q. Microstructure and mechanical properties of Ni$_3$Al and Ni$_3$Al−1B alloys fabricated by SHS/HE [J]. Intermetallics, 2011, 19(2): 137−142.

[13] LEBRAT J P, VARMA A. Self-propagating high-temperature synthesis of Ni$_3$Al [J]. Combust Sci Technol, 1992, 88(3−4): 211−221.

[14] HIBINO A, MATSUOKA S, KIUCHI M. Synthesis and sintering of Ni$_3$Al intermetallic compound by combustion synthesis process [J]. J Mater Process Technol, 2001, 112(1−3): 127−135.

[15] SHENG L Y, ZHANG W, GUO J T, WANG Z S, OVCHARENKO V E, ZHOU L Z, YE H Q. Microstructure and mechanical properties of Ni$_3$Al fabricated by thermal explosion and hot extrusion [J]. Intermetallics, 2009, 17(7): 572−577.

[16] DUTTA B, PALMIERE E J, SELLARS C M. Modelling the kinetics of strain induced precipitation in Nb microalloyed steels [J]. Acta Mater, 2001, 49: 785−794.

[17] SHENG L Y, XIE Y, XI T F, GUO J T, ZHENG Y F, YE H Q. Microstructure characteristics and compressive properties of NiAl-based multiphase alloy during heat treatments [J]. Materials Science and Engineering A, 2011, 518: 8324−8331.

[18] SHENG L Y, WANG L J, XI T F, ZHENG Y F, YE H Q. Microstructure, precipitates and compressive properties of various holmium doped NiAl/Cr(Mo, Hf) eutectic alloys [J]. Mater Design, 2011, 32(10): 4810−4817.

[19] SCHULSON E M, WEIHS T P, VIENS D V, BAKER I. The effect of grain size on the yield strength of Ni$_3$Al [J]. Acta Metall, 1985, 33(9): 1587−1591.

[20] TAKEYAMA M, LIU C T. Effects of grain size and test temperature on ductility and fracture behavior of A B-doped Ni$_3$Al alloy [J]. Acta Metall, 1988, 36(5): 1241−1249.

[21] SHENG L Y, ZHANG W, GUO J T, ZHOU L Z, YE H Q. Microstructure evolution and mechanical properties improvement of NiAl−Cr(Mo)−Hf eutectic alloy during suction casting and subsequent HIP treatment [J]. Intermetallics, 2009, 17(12): 1115−1119.

[22] WUNDERLICH W, KREMSER T H, FROMMEYER G. Mobile dislocations at the α_2/γ phase boundaries in intermetallic TiAl/Ti$_3$Al-alloys [J]. Acta Metall Mater, 1993, 41(6): 1791−1799.

[23] KORZNIKOV A V, TRAM G, DIMITROV O, KORZNIKOVA G F, IDRISOVA S R, PAKIELA Z. The mechanism of nanocrystalline structure formation in Ni$_3$Al during severe plastic deformation [J]. Acta Mater, 2001, 49(4): 663−671.

高温自蔓延过程中的挤压工艺对合成 Ni$_3$Al−B−Cr 合金的组织及力学性能的影响

盛立远[1,2]，奚廷斐[1]，赖 琛[1]，郭建亭[3]，郑玉峰[2]

1. 北京大学−香港科技大学 深圳研修院，深圳 518057；
2. 北京大学 工学院，北京 100871；
3. 中国科学院 金属研究所，沈阳 110016

摘　要：采用高温自蔓延及挤压工艺制备 Ni$_3$Al−0.5B−5Cr 合金，研究挤压工艺对合成合金的微观组织及力学性能的影响。结果表明：合成后的挤压工艺可使合成合金进一步致密并能有效地细化其组织。X 射线衍射及透射电镜观察发现除了 Ni$_3$Al 基体外，合金中还含有 Al$_2$O$_3$、Ni$_3$B 及 Cr$_3$Ni$_2$ 析出相。与无挤压合成的合金有所不同，合金在高温自蔓延合成及挤压过程中经历了大变形和再结晶过程，其促进了组织的细化并降低了晶粒的取向差。此外，合成后的挤压工艺促使 Al$_2$O$_3$ 颗粒重新分布且减少了 γ-Ni 相。与无挤压合成的合金相比，高温自蔓延合成及挤压工艺制备的合金具有更好的室温力学性能。

关键词：Ni$_3$Al 金属间化合物；高温自蔓延合成；挤压；微观组织；力学性能

(Edited by LI Xiang-qun)